Blazar Population Estimates

Chuck Dermer
U.S. Naval Research Laboratory

GLAST DCII AGNLATSG F2F 04032006 10:00 SLAC CA USA

Stanley P. Davis
GSFC, Lincoln U

Truong Le
NRL

History

1991: 1 γ-ray blazar: 3C273

5 April 1991: Launch of GRO

1992: γ-ray blazar class: 3C 279, 3C 273, PKS 0528+134…

1995: 40/51 EGRET blazars

2EG, Thompson et al. (1995)
von Montigny et al. (1995)
Mukherjee et al. (1997)

The EGRET

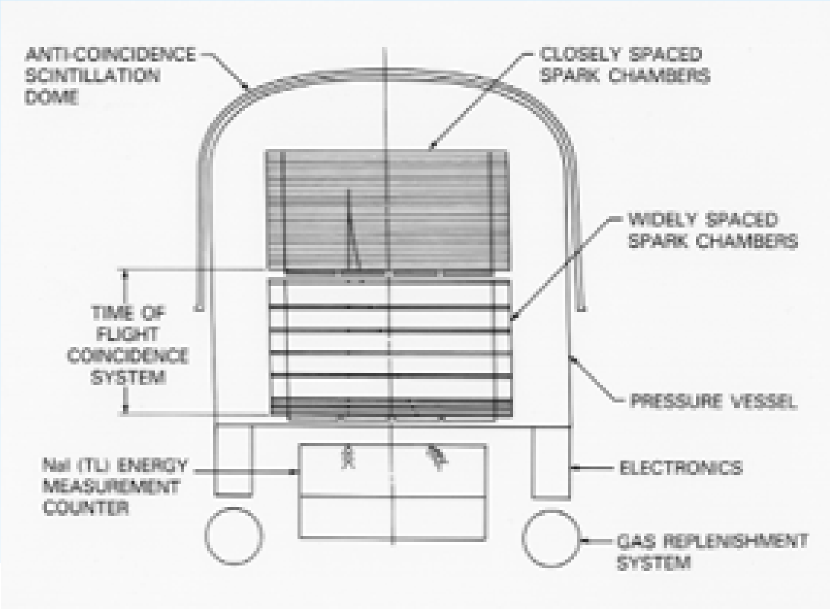

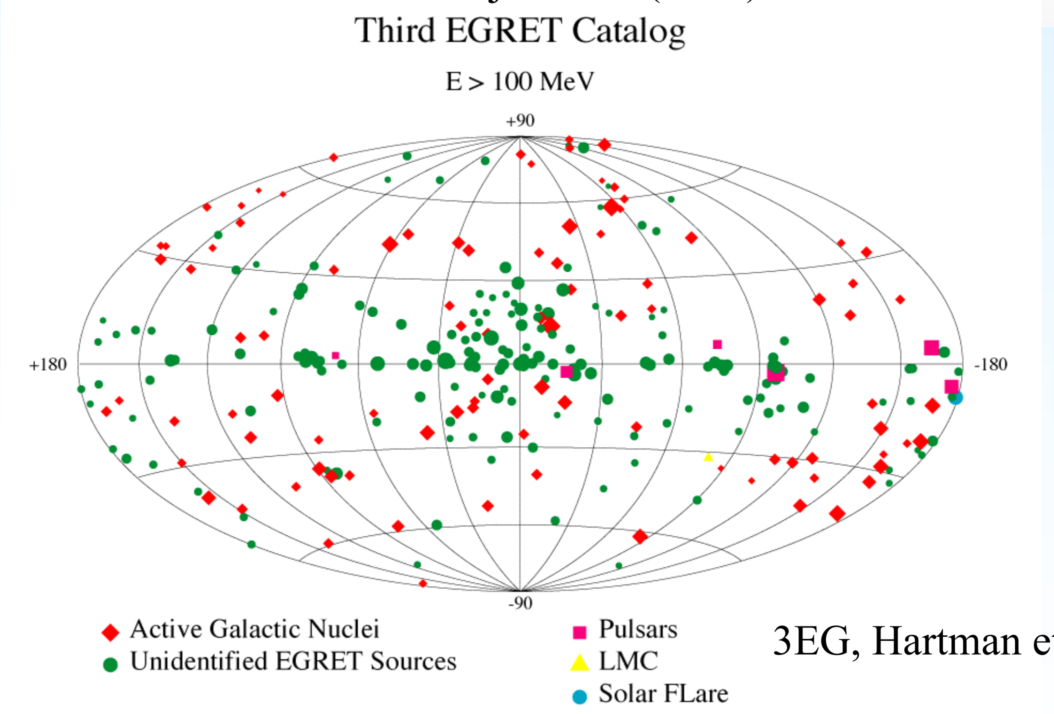

3EG, Hartman et al. (1999)

Relativistically beamed emission:
superluminal sources
radio connection
Flat Spectrum radio sources
Kuehr catalog
blazars (incl. LBLs and HBLs)
Blue blazar/TeV connection

γ-ray Population Studies

Stecker and Salamon (1996)
assuming radio-γ correlation

(see also talk by Paolo Giommi)

RLF

$$\rho_r(P_r, z) = 10^{-8.15}\left\{\left[\frac{P_r}{P_c(z)}\right]^{0.83} + \left[\frac{P_r}{P_c(z)}\right]^{1.96}\right\}^{-1}$$

γLF

$$\rho_\gamma(P_{\gamma f}, z) = (1-\zeta)\eta\rho_r\left(\frac{P_{\gamma f}}{\kappa}, z\right) + \zeta\eta\rho_r\left(\frac{P_{\gamma f}}{A\kappa}, z\right)$$

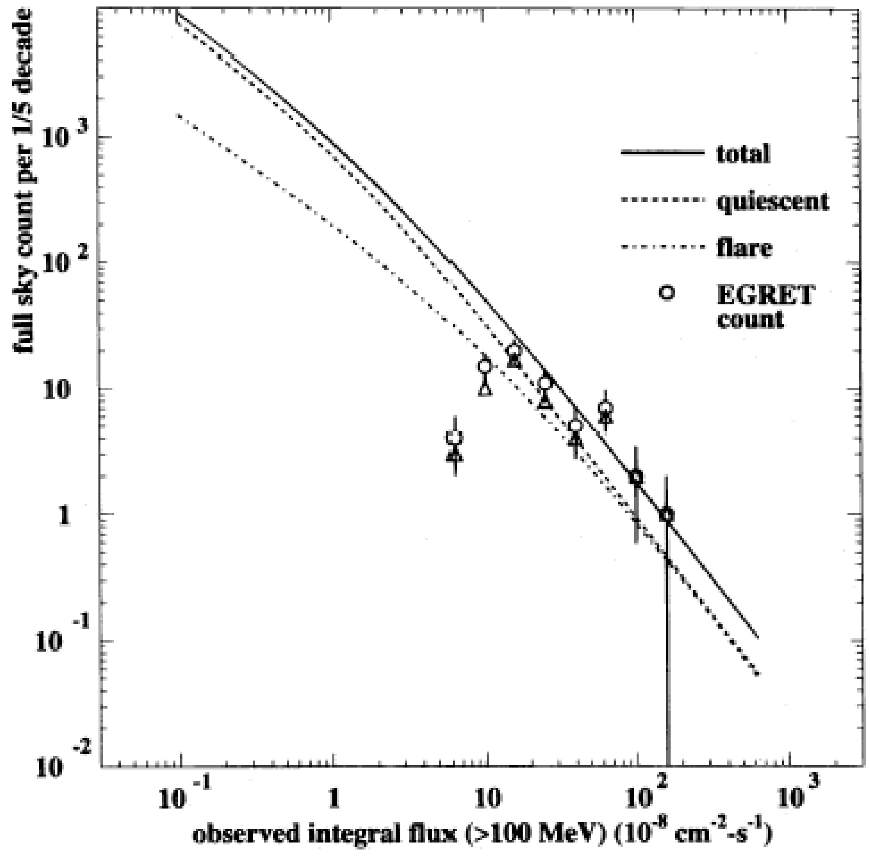

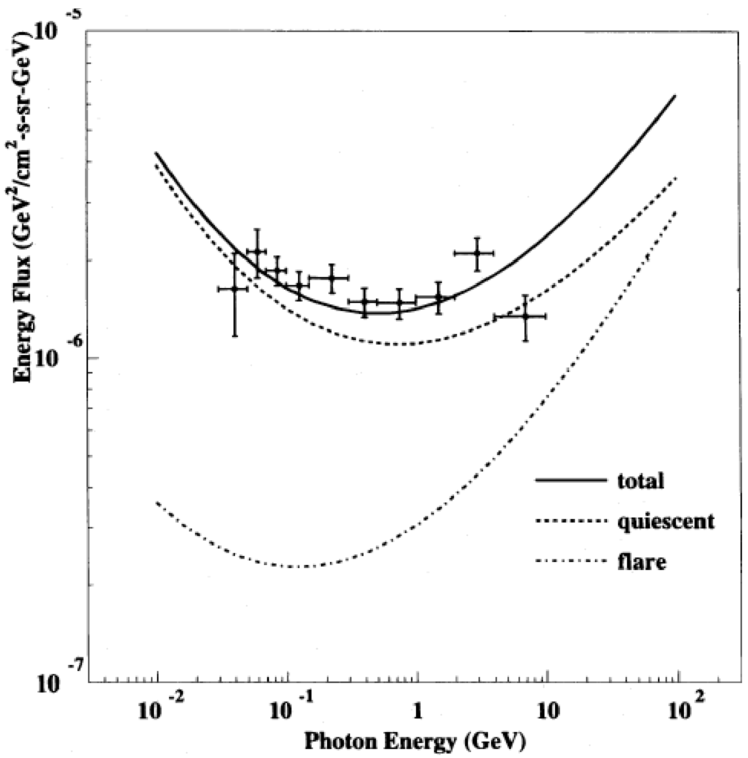

γ-ray Population Studies with Luminosity Evolution

Chiang et al. (1995)
Chiang and Mukherjee (1997)

Narumoto and Totani (2005)
Giommi and Colafrancesco (2006)

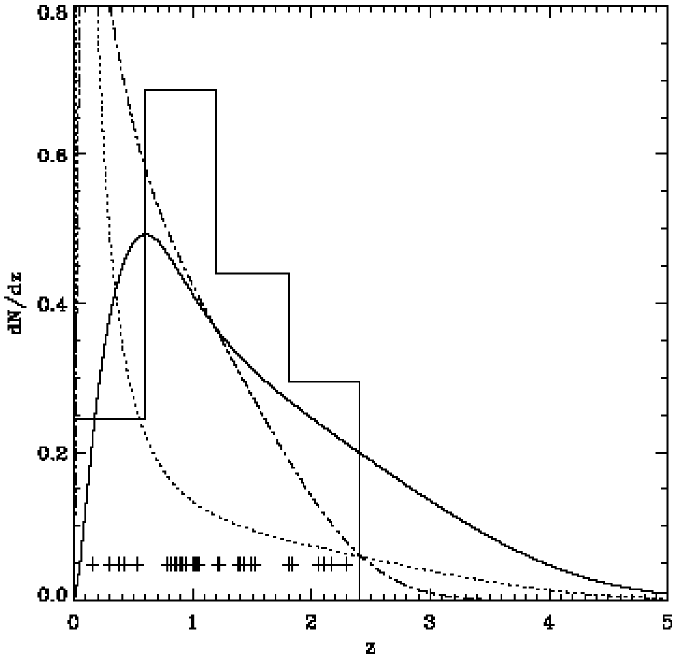

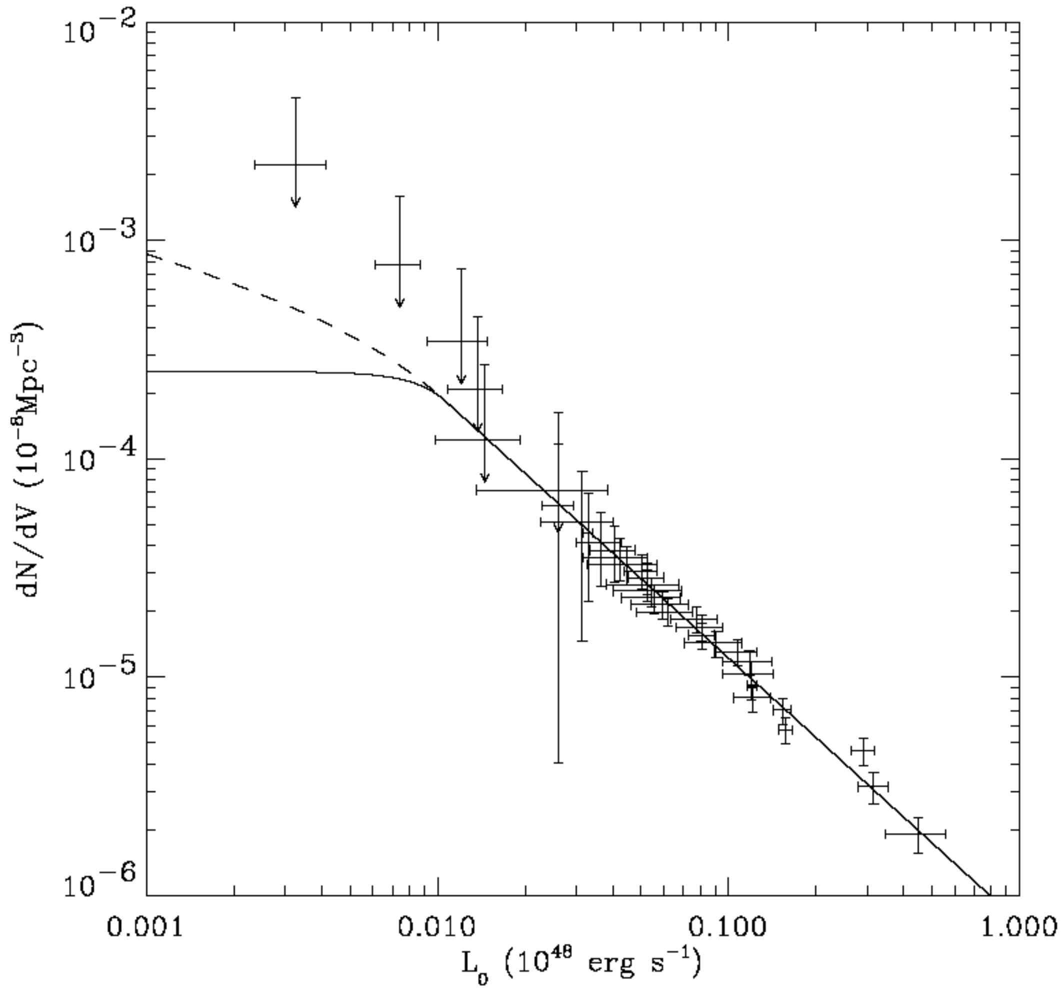

3C 279 Variability

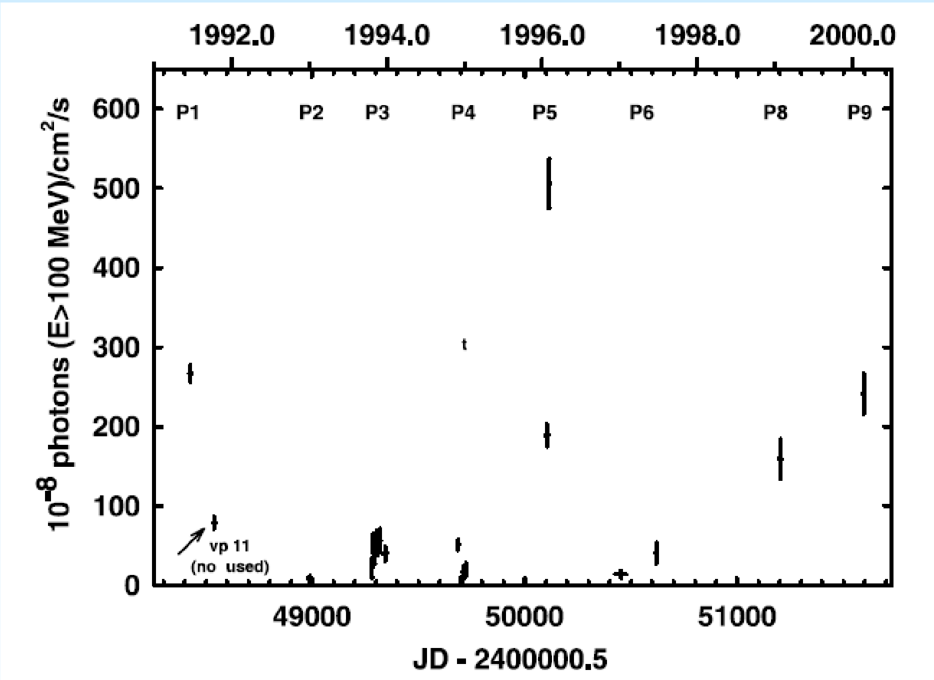

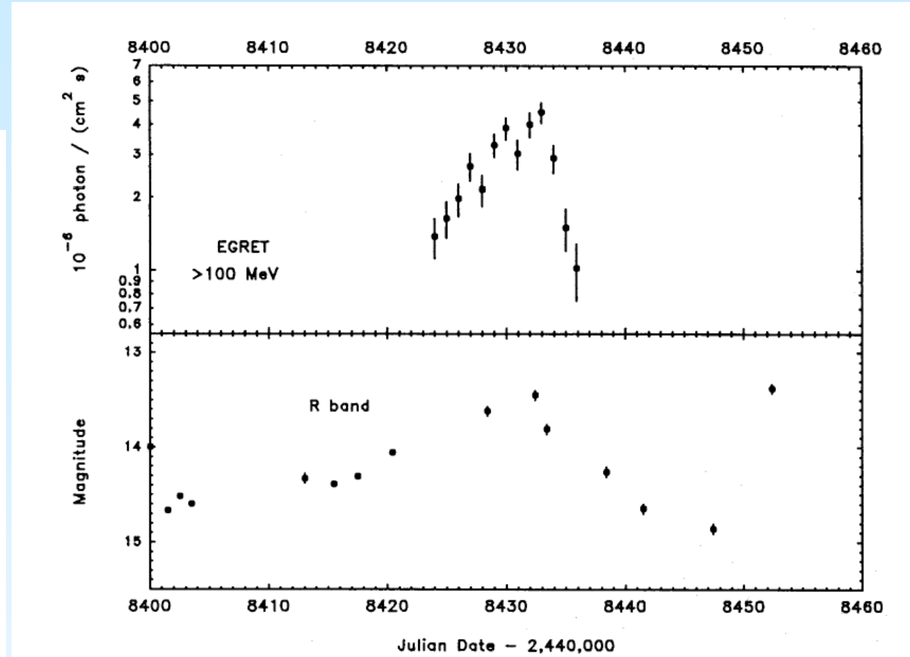

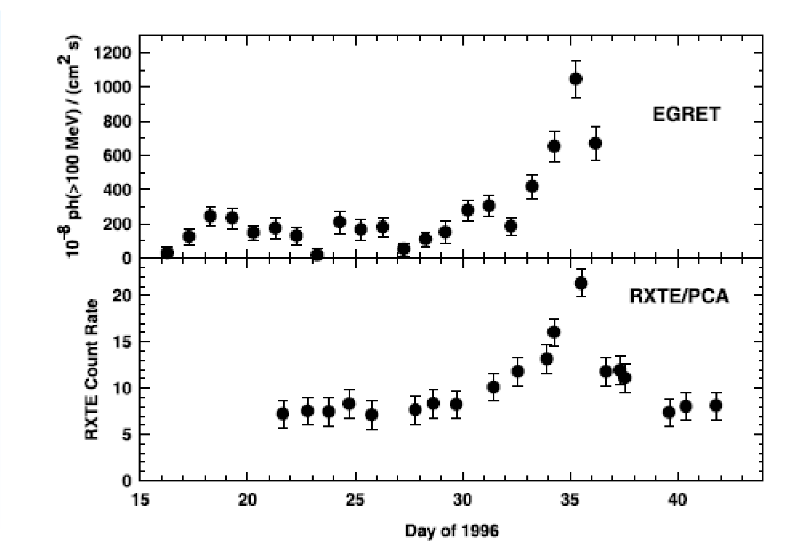

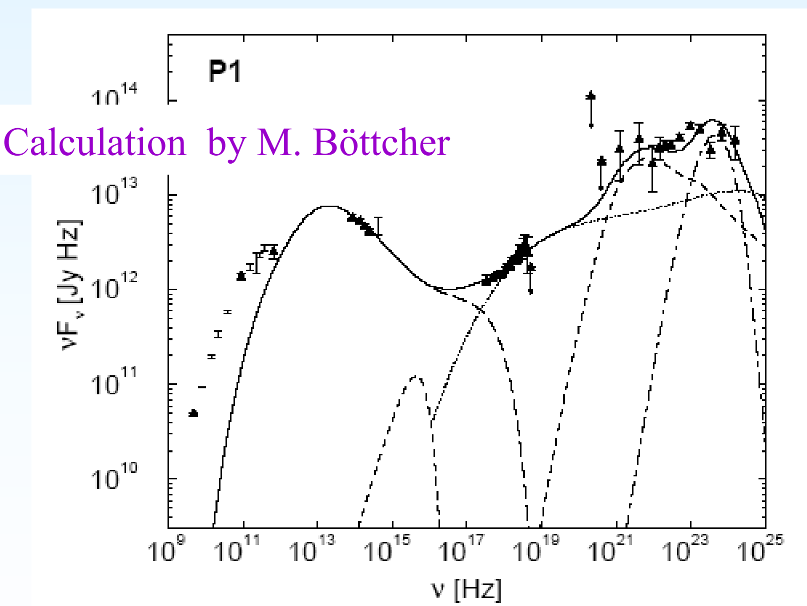

Calculation by M. Böttcher

Hartman et al. 1992, 1996, 2000

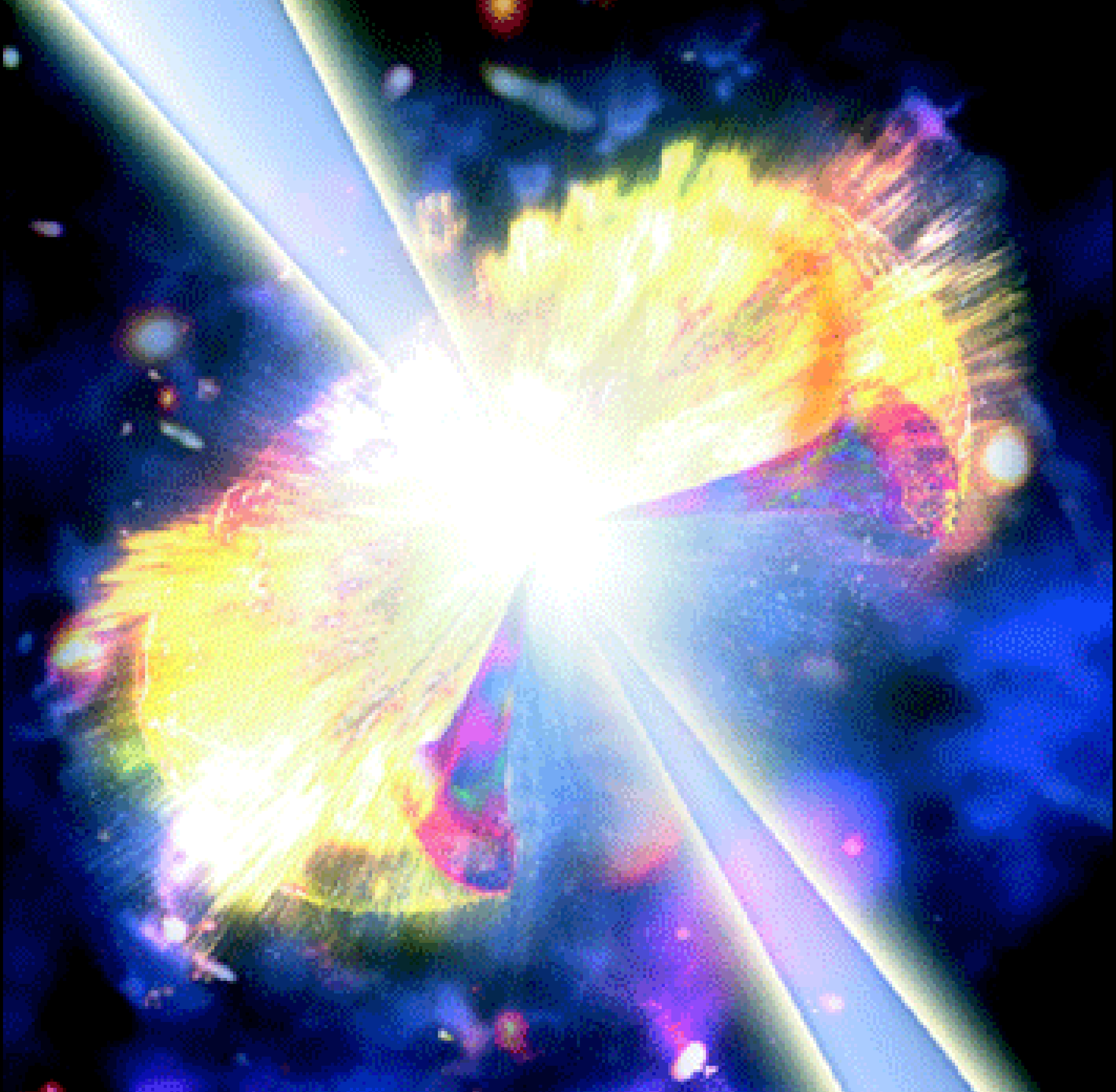

Physical Model

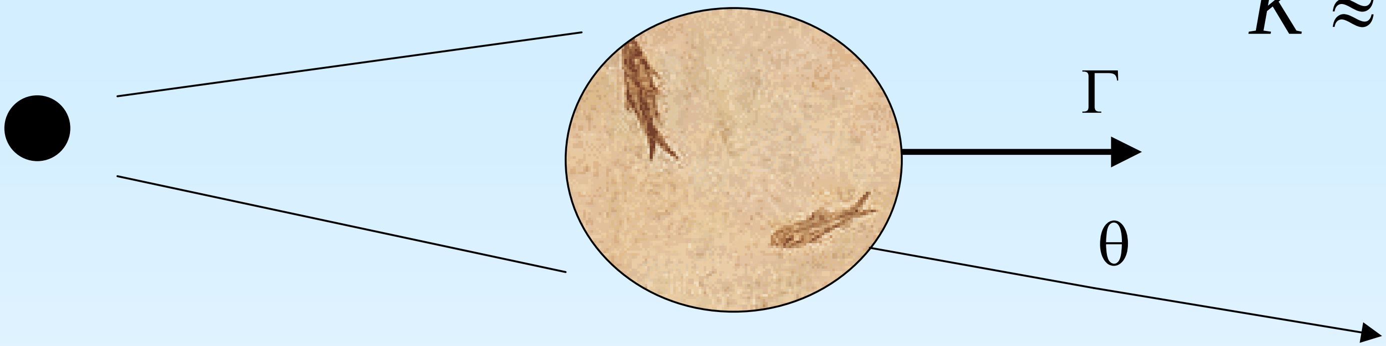

$$K \approx \frac{(p-2)W'_e}{m_e c^2 \gamma_1^{2-p}}$$

$$Power-law\ \ electron\ \ distribution:$$

$N'_e(\gamma) = K\gamma^{-p} H(\gamma;\gamma_1,\gamma_2); W'_e =$ nonthermal electron energy

$$\boxed{f_{\varepsilon}^{proc} \cong \frac{\ell'_e}{d_L^2}\delta_D^q \varepsilon_z^{(3-p)/2}}$$

Nonthermal Radiation Physics of Jets: Synchrotron Emission

Stationary: *
Comoving: ′
Observer:

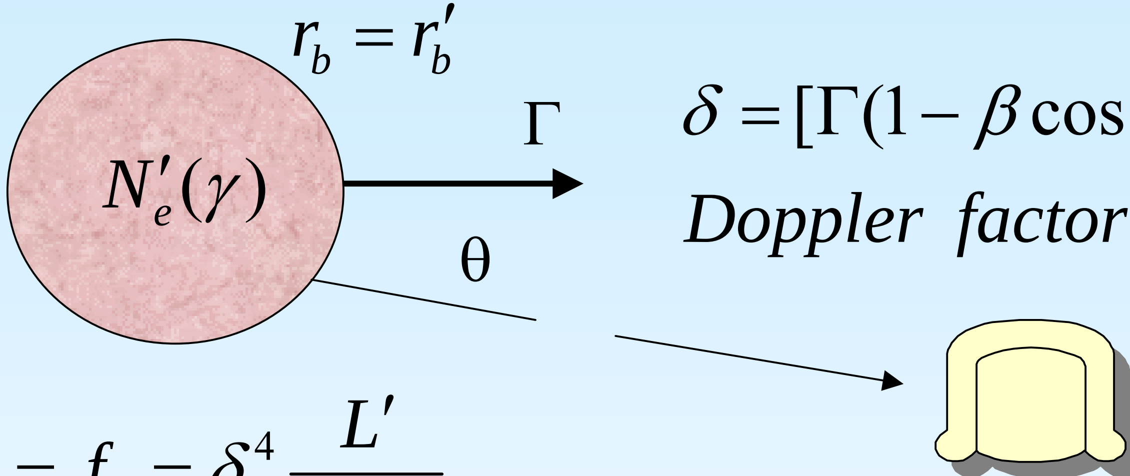

$\delta = [\Gamma(1-\beta\cos\theta)]^{-1}$

Doppler factor

$$\nu F_\nu = f_\varepsilon = \delta^4 \frac{L'}{4\pi d_L^2}$$

$$\boxed{\nu F_\nu = f_\varepsilon^{\,syn} = \frac{\delta^4}{d_L^2}\varepsilon' J(\varepsilon',\Omega') \cong \frac{\delta^4}{6\pi d_L^2} c\sigma_T u_B \gamma_s^3 N_e'(\gamma_s)\,,}$$

$$\gamma_s = \sqrt{\frac{(1+z)\varepsilon}{\delta(B/B_{cr})}}$$

$u_B = B^2/8\pi$

$B_{cr} = m_e^2 c^3 / e\hbar$

Critical magnetic field

q = (p+5)/2

External Compton (EC)

target photon energy $\varepsilon_* = h\nu_*/m_e c^2$

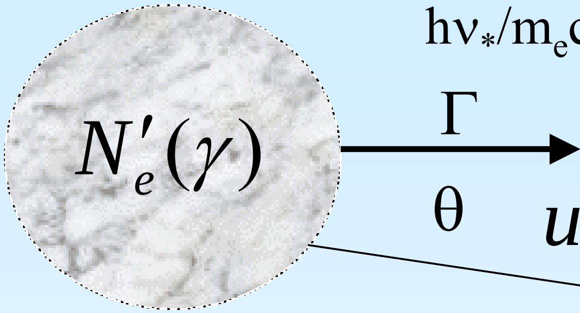

$$u' \cong \Gamma^2 u_*$$

$$FSRQ: u_* \sim ergs\ cm^{-3}$$

q = p+3

$$\varepsilon_* \cong 10^{-4} M_8^{-1/4}$$

$$CMBR:\ u_* = 4\times 10^{-13}(1+z)^4\ ergs\ cm^{-3},\ \varepsilon_* \cong 1.3\times 10^{-9}(1+z)$$

$$\boxed{\nu F_\nu = f_\varepsilon^{EC} \cong \frac{\delta^6}{6\pi d_L^2} c\sigma_T u_* \gamma_{EC}^3 N_e'(\gamma_{EC})}$$

$$\gamma_{EC} = \frac{1}{\delta}\sqrt{\frac{(1+z)\varepsilon}{2\varepsilon_*}}$$

$$f_{\varepsilon_S}^{EC} / f_{\varepsilon_{EC}}^{syn} \propto \delta_D^{(p+1)/2} \propto \delta_D^{1+\alpha}$$

CD (1995), DSS (1997)

Synchrotron self-Compton (SSC)

$$n'_{syn}(\varepsilon') \approx \frac{\dot{N}_{syn}(\varepsilon')}{4\pi r_b^2 c}$$

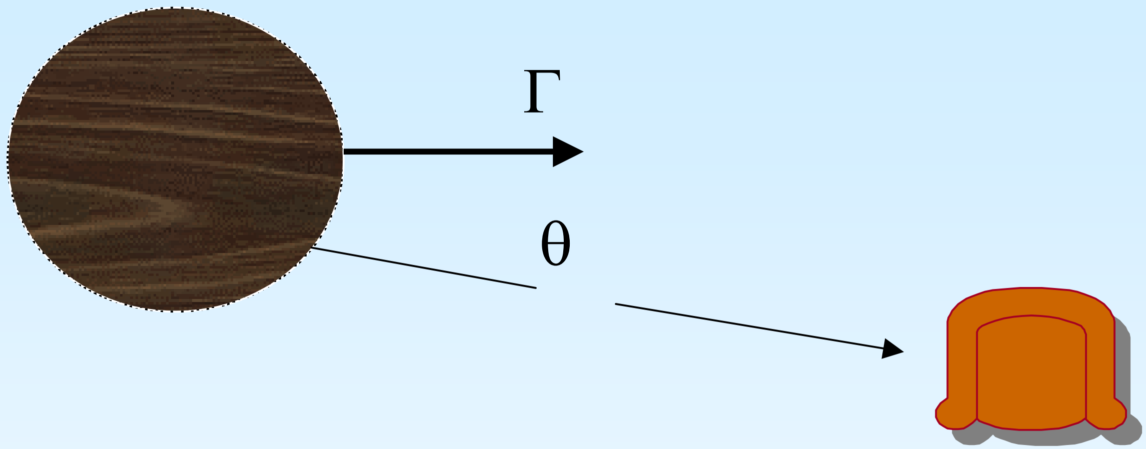

$$\boxed{\nu F_\nu = f_\varepsilon^{SSC} \cong \frac{\delta^4}{9\pi d_L^2} \frac{c\sigma_T^2 r_b u_B K^2}{V'_b} \gamma_s^{3-p} \Sigma_C}$$

$$f_\varepsilon^{SSC} \propto \delta^{(5+p)/2} B^{(9+p)/2} \varepsilon_z^{(3-p)/2}$$

Same beaming factor as synchrotron

Density and Luminosity Evolution of IR galaxies: 30 – 300μ (900 GHz)

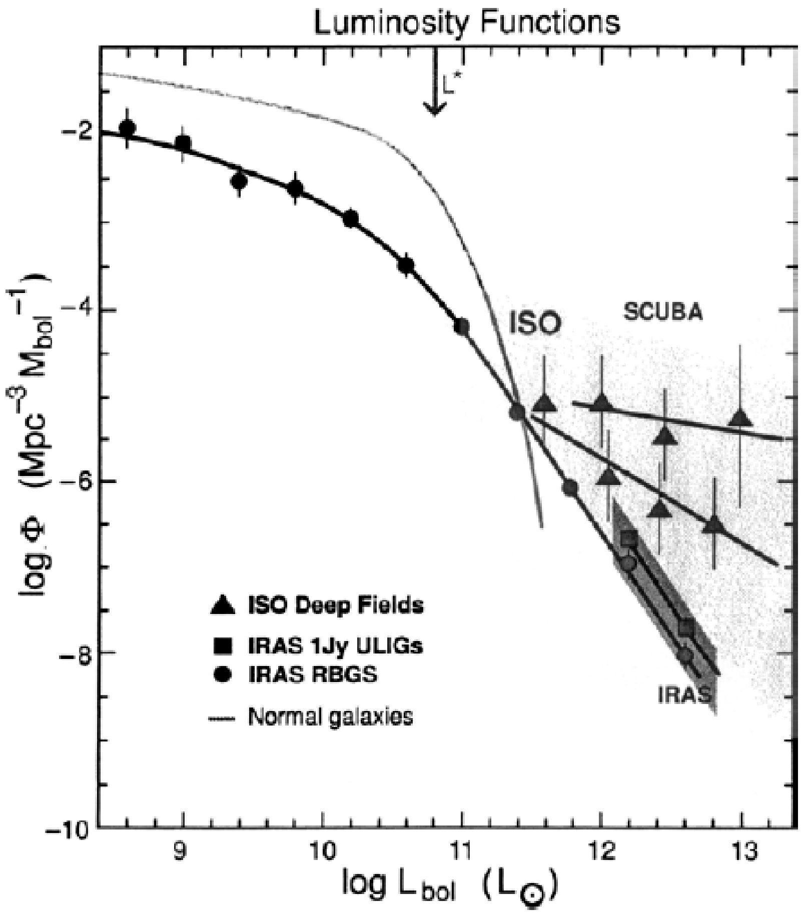

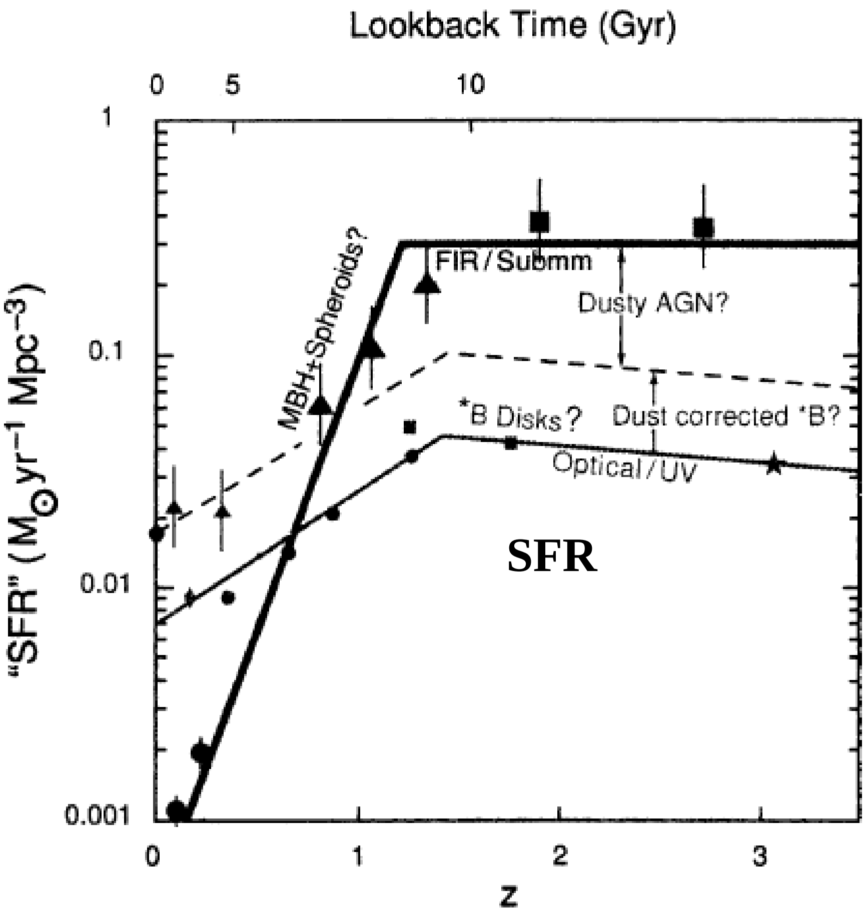

Sanders (2004)

Analytic Blazar Formation Rate

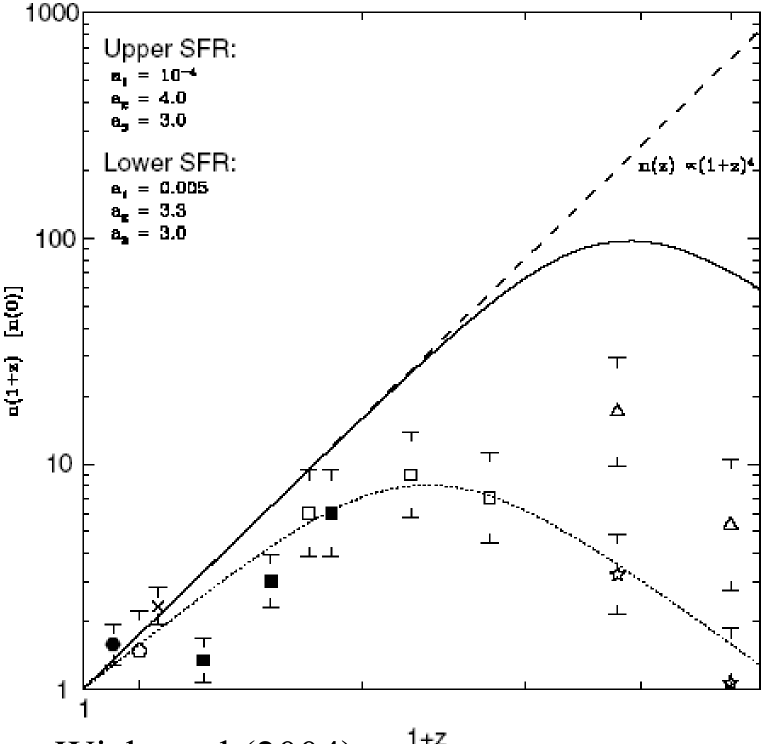

Wick et al (2004)

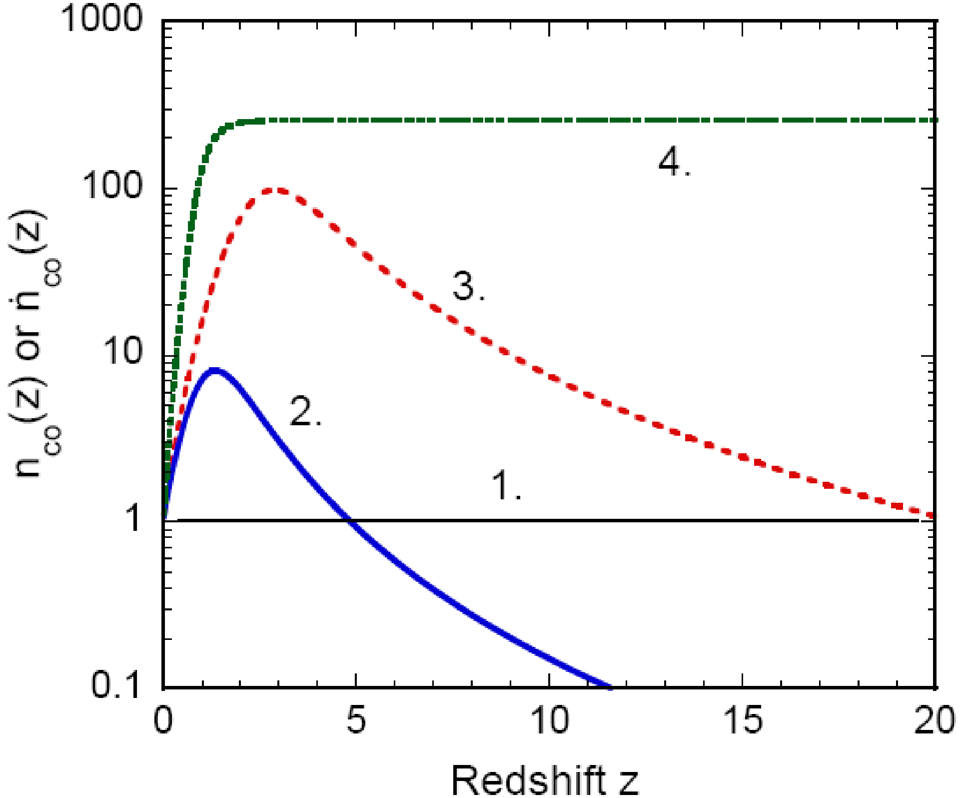

1. Constant Comoving Density
2. “Madau” curve
3. SFR with extinction corrections
4. Evolution of IR from IR galaxies

Simple analytic forms

Blazar Main Sequence

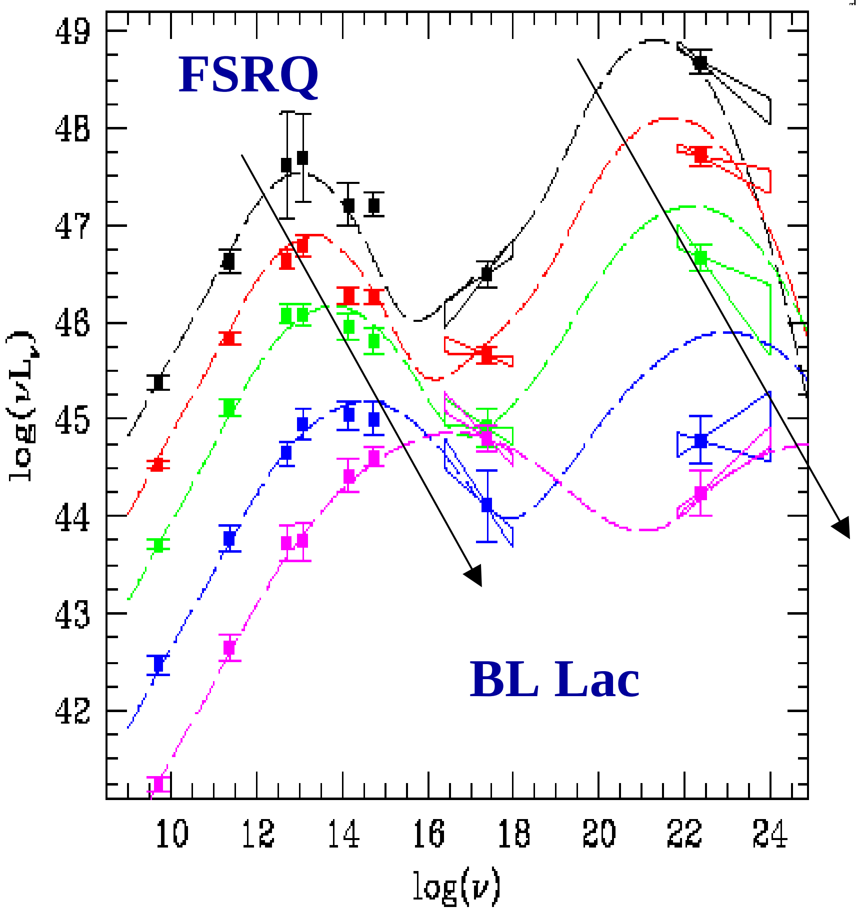

Sambruna et al. (1996); Fossati et al. (1998)

Flaring vs. quiescent behavior

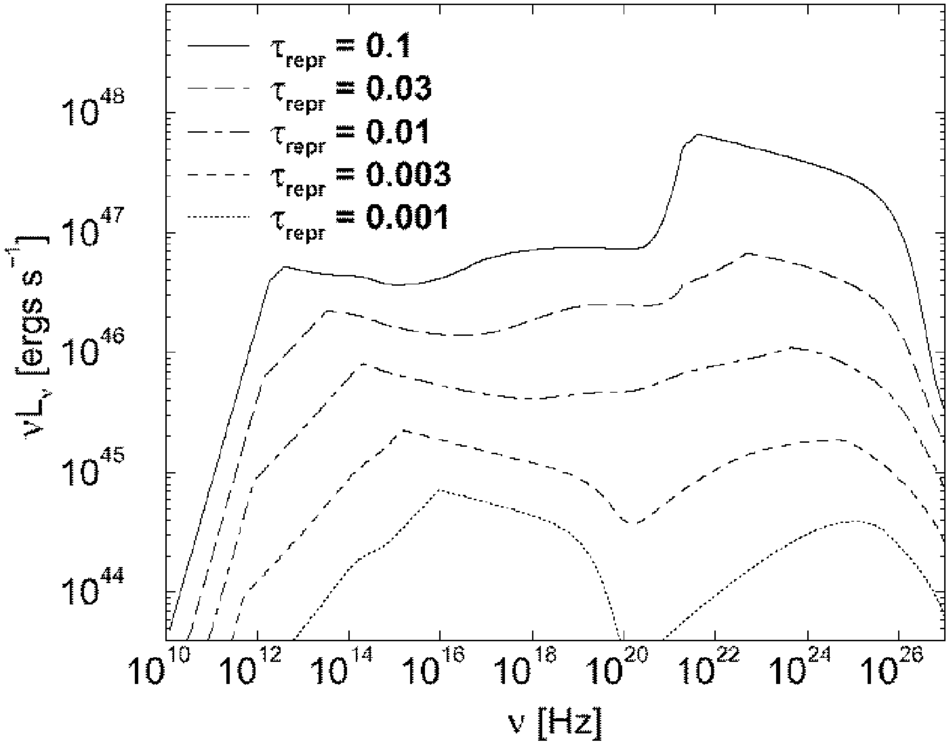

Evolution from FSRQ to BL Lac Objects in terms of a reduction of fuel from surrounding gas and dust

Böttcher and Dermer (2000)
Cavaliere and d'Elia (2000)

Observed redshift distribution of blazars

Redshift distribution of EGRET blazars (histograms), separated into 46 FSRQs and 14 BL Lac Objects (BLs).

Uniform exposure: EGRET all-sky survey

Fichtel et al. (1994): 1EG

GLAST: essentially uniform exposure

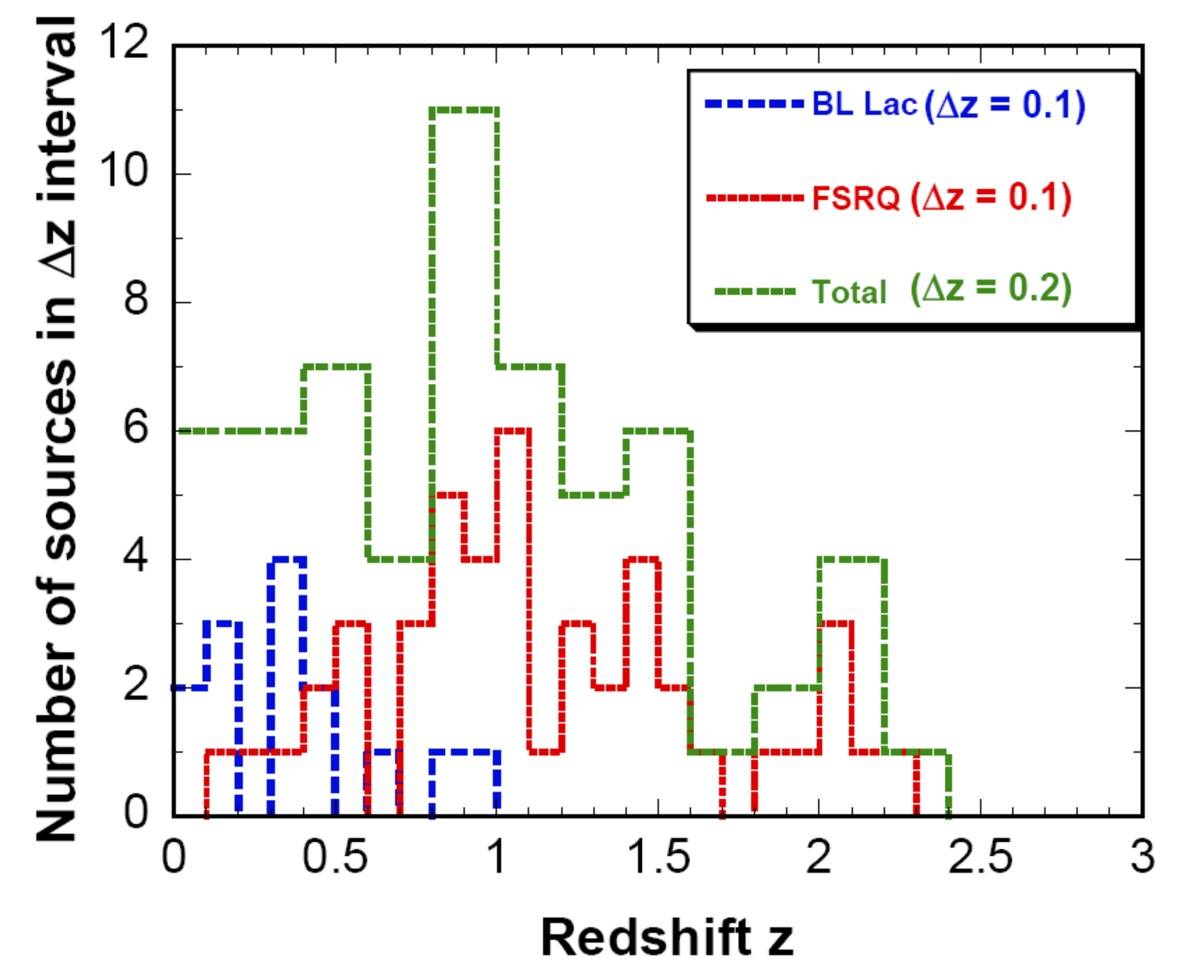

(Peak) flux distribution of EGRET Blazars

Histogram showing the measured peak power flux size distribution of EGRET blazars, separated into FSRQs and BLs

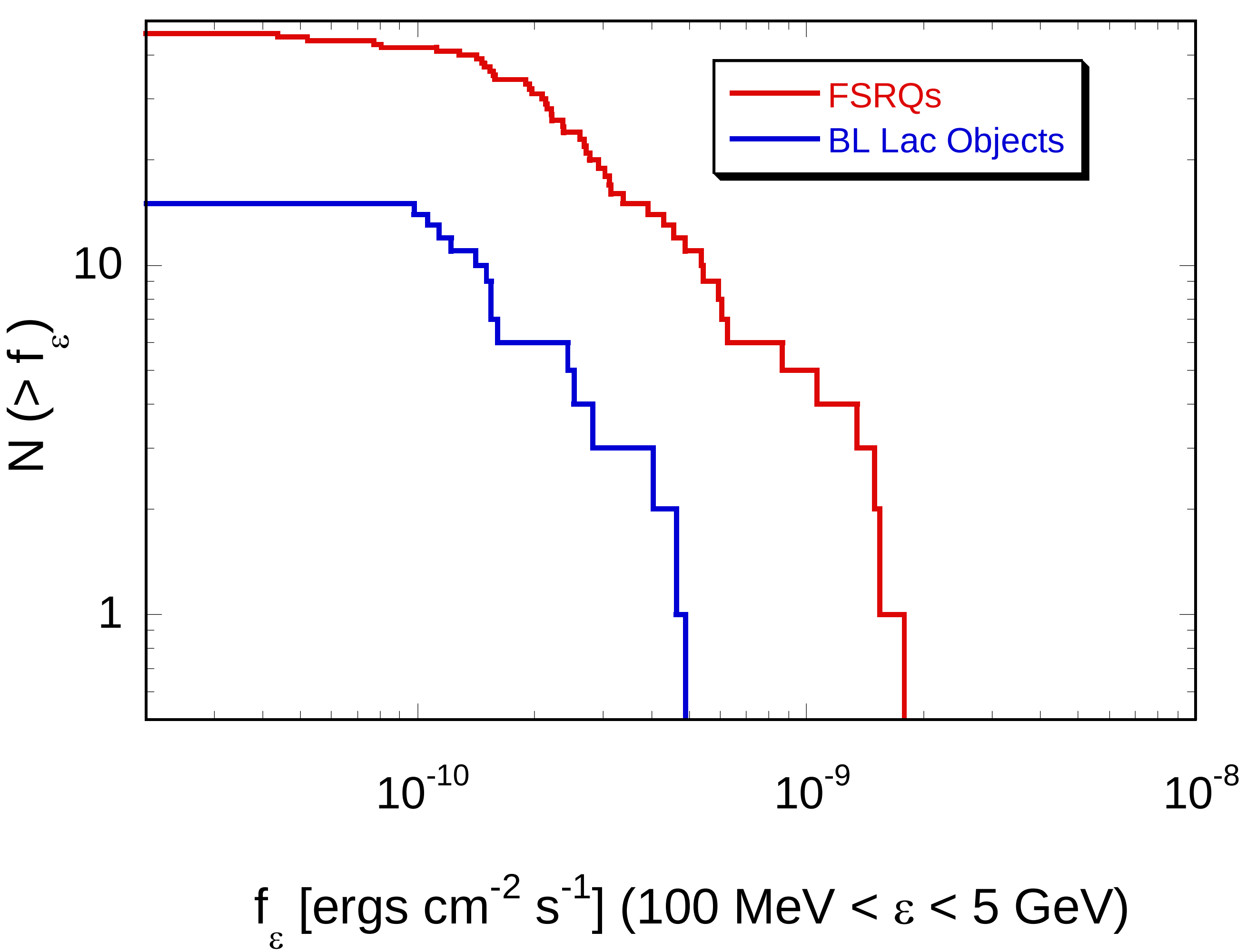

Measured γ-ray blazar peak luminosity distribution

Distribution of observed peak luminosities of FSRQs and BLs as measured in the EGRET energy range.

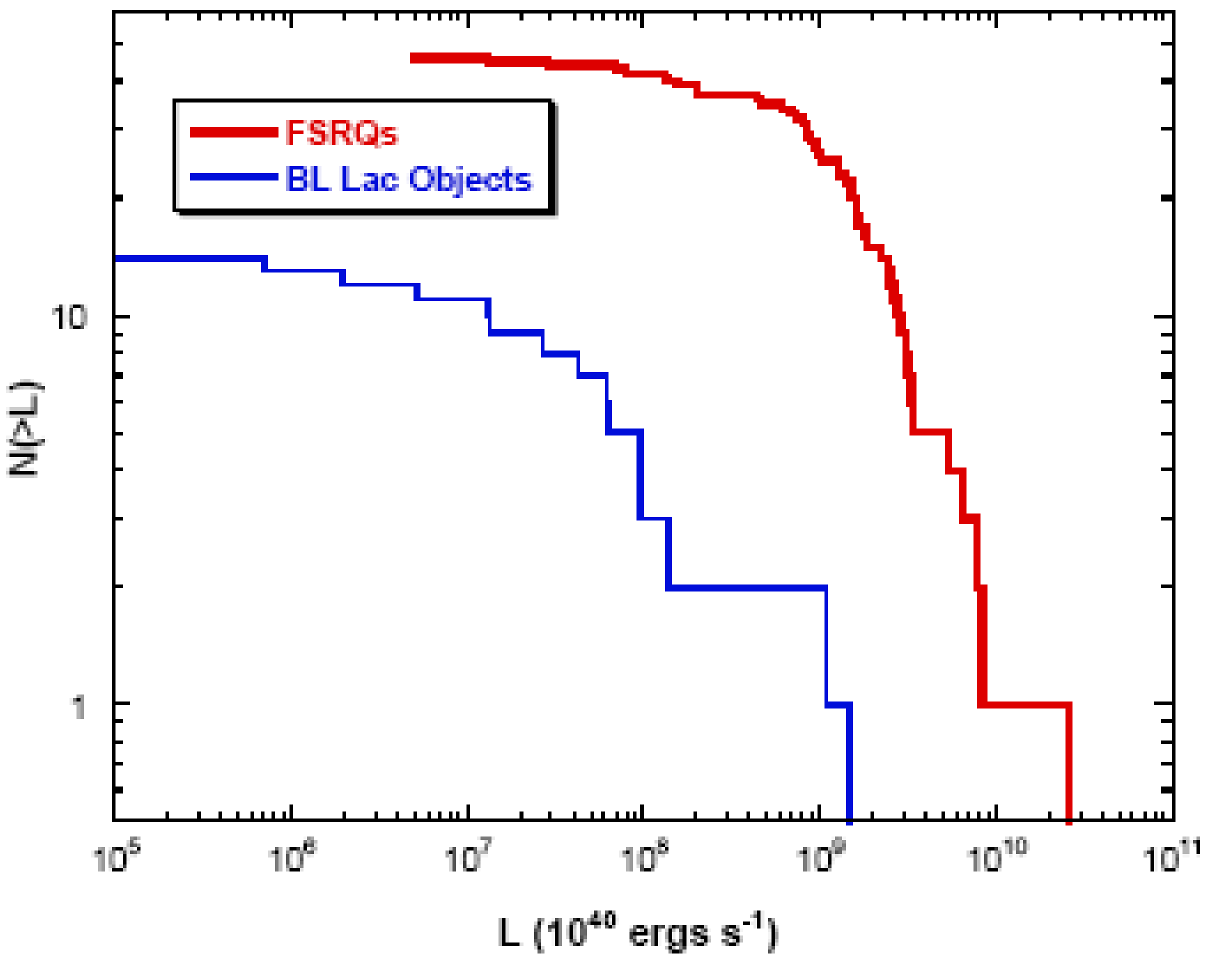

Statistics of cosmological relativistic jet sources

ΛCDM cosmology, bursting sources

$$\frac{d\dot{N}}{d\Omega} = \frac{c}{H_0}\frac{d_L^2\ \dot{n}_{co}(L_*, \alpha; z)dL_* d\alpha dz}{(1+z)^3\ \sqrt{\Omega_m(1+z)^3+\Omega_\Lambda}}$$

$\hat{f}_{\bar{\varepsilon}} : \nu F_\nu$ *flux threshold*

$\hat{f}_{\bar{\varepsilon}} \approx 2\times 10^{-11}\ ergs\ cm^{-2}\ s^{-1}: \quad EGRET$ $\quad$ $\hat{f}_{\bar{\varepsilon}} \approx (1-5)\times 10^{-13}\ ergs\ cm^{-2}\ s^{-1}: \quad GLAST$

$\bar{\varepsilon} \approx 200$ $\quad$ $\bar{\varepsilon} \approx 200-2000$

Redshift distribution above f_ε

$$\frac{d\dot{N}}{dz d\Omega}(> f_\epsilon) = \frac{c}{H_0}\frac{d_L^2(z)\ \dot{n}_{co}(z)}{(1+z)^3\ \sqrt{\Omega_m(1+z)^3+\Omega_\Lambda}}[1-\max(0,\hat{\mu}(z))]$$

Integrate over z to get f_ε flare size distribution: p for spectrum, q for beaming factor

$$\hat{\mu}(z) = \frac{1}{\beta}\left\{1-\frac{1}{\Gamma}\left[\frac{\ell'_e \epsilon_z^{(3-p)/2}}{d_L^2(z) f_\epsilon}\right]^{1/q}\right\}$$

Redshift distribution of model γ-ray blazars: BFH

Histogram showing the model redshift distributions of EGRET blazars, assuming constant comoving density of blazars and an $\Omega_m = 0.3$, $\Omega_\Lambda = 0.7$ cosmology with a Hubble constant $H_0 = 72$ for different blazar formation histories (BFHs)

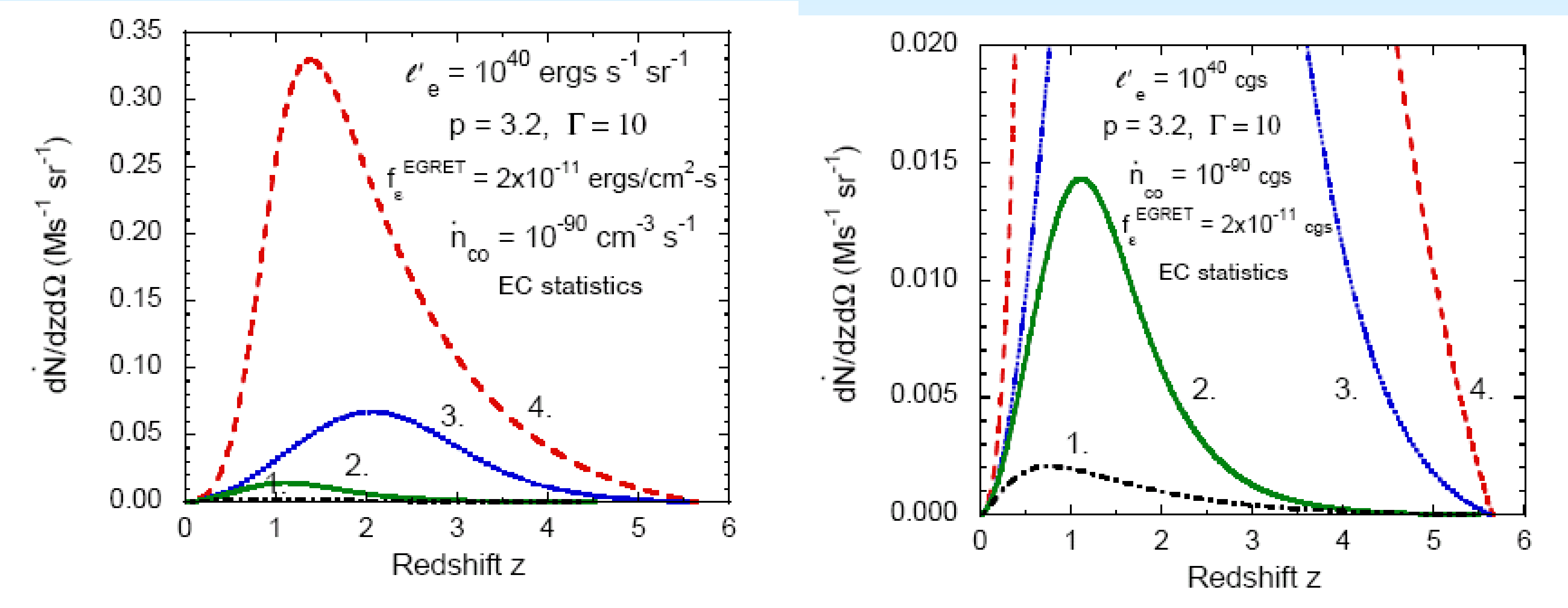

Fig. 4.— Variation in the blazar redshift distribution above an EGRET-type sensitivity threshold $= 2 \times 10^{-11}$ ergs cm^{-2} s^{-1} at $\epsilon \approx 200$ for different blazar formation histories (BLHs). The linear scale on the left shows better BFH3 and 4 (left), and on the right shows better BFH 1 and 2, for standard model blazar with parameters indicated.

Redshift distribution of model γ-ray blazars: ℓ'_e

Changing comoving directional luminosity.

Standard value is: $\ell'_e : \; 10^{40} \; ergs \; s^{-1} \; sr^{-1}$

Note that BFH3 gives a peak redshift <z> ~ 2 rather than <z> ~ 1 (observed) unless ℓ'_e or Γ are small

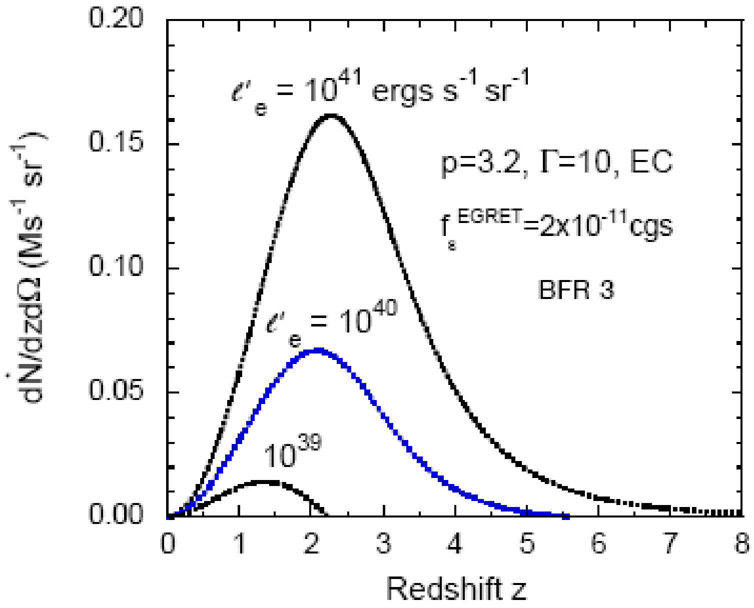

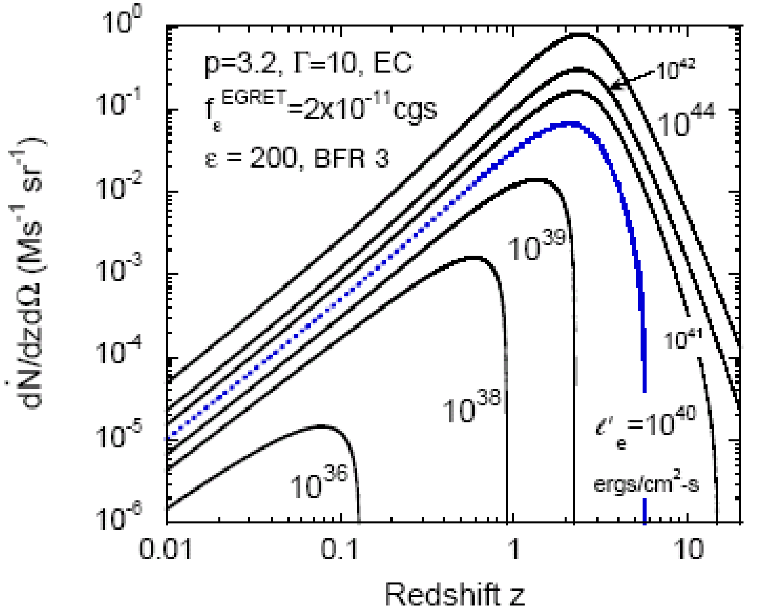

Fig. 5.— Model redshift distributions for standard model blazars with only the comoving power changed, assuming a blazar formation history proportional to the star formation rate history with extinction corrections, BFH 3. (left) On a linear scale, with ℓ'_e changed by only 2 orders of magnitude. (right) On a log-log scale, with ℓ'_e changed by 8 orders of magnitude.

Redshift distributions of model γ-ray blazars: Γ

Changing Γ factor: standard value is 10; BFR 3

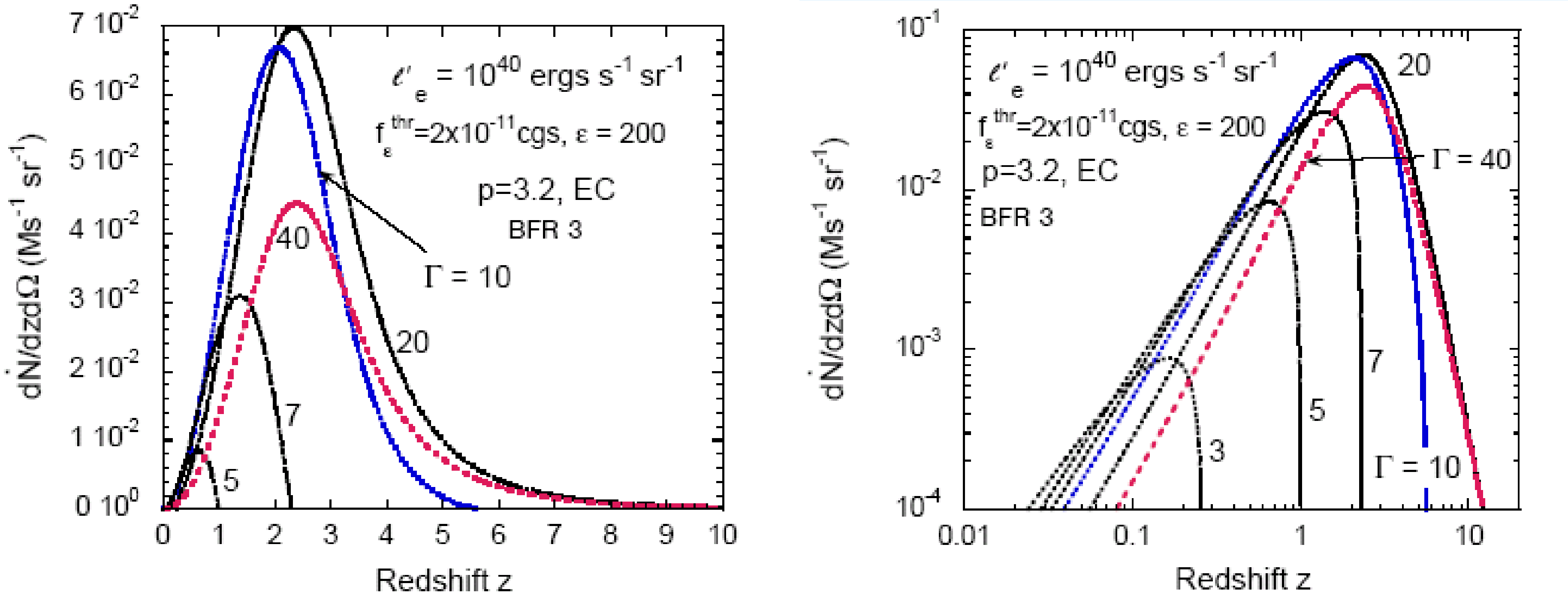

Fig. 6.— Blazar redshift distribution for a model blazar with Γ varied from 3 – 40, for EGRET detection properties, with a νF_ν threshold sensitivity of 2×10^{-12} ergs cm^{-2} s^{-1} at $\epsilon = 200$. (left) Linear scale. (right) Logarithmic scale.

Redshift distribution of model γ-ray blazars: beaming factor

Note different directional luminosities and Γ factors

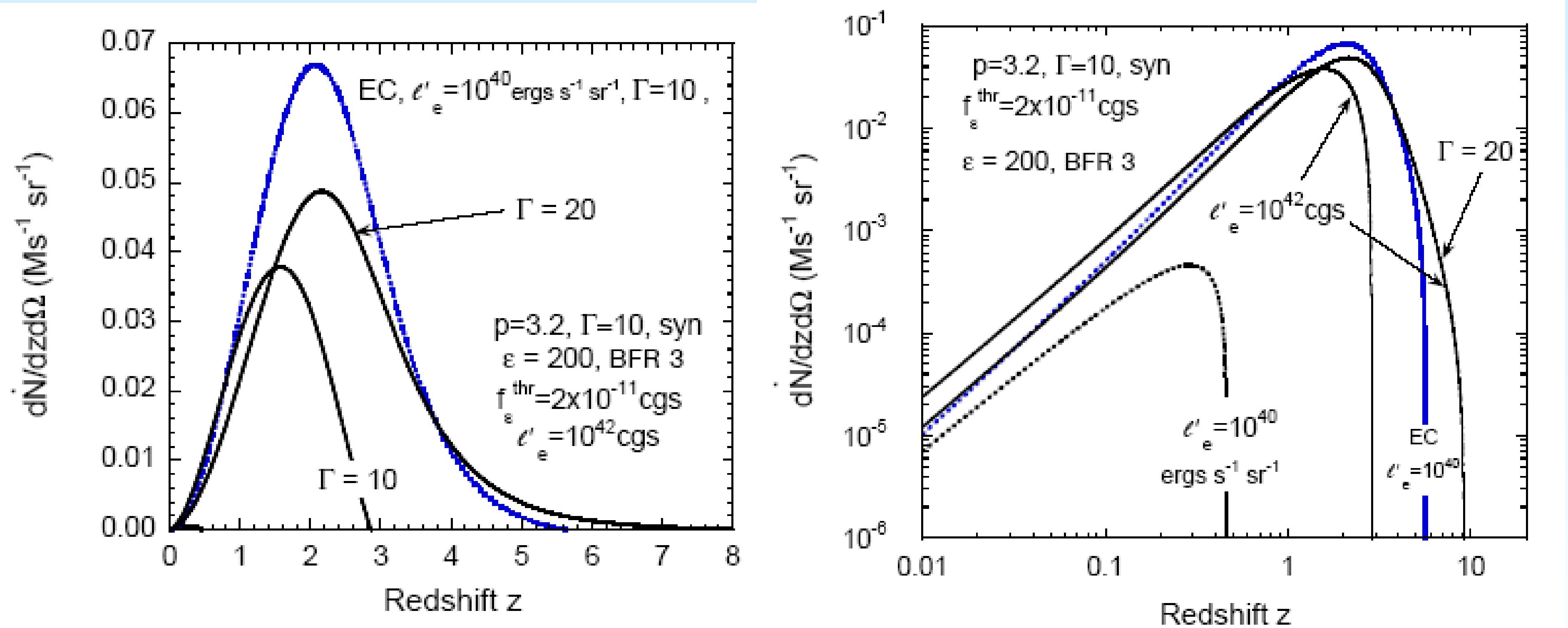

Fig. 7.— Blazar redshift distribution for a model blazar with Γ = 10, EC statistics, and EGRET detection properties (upper blue dotted curve) compared with results for synchrotron statistics, with different directional jet powers ℓ'_ε and Γ factors as labeled. (left) Linear scale. (Right) Logarithmic scale.

Preliminary predictions for FSRQs

Standard model blazar, Γ = 10, EC, directional luminosity of 10^{40} ergs s^{-1} sr^{-1}, different BFHs

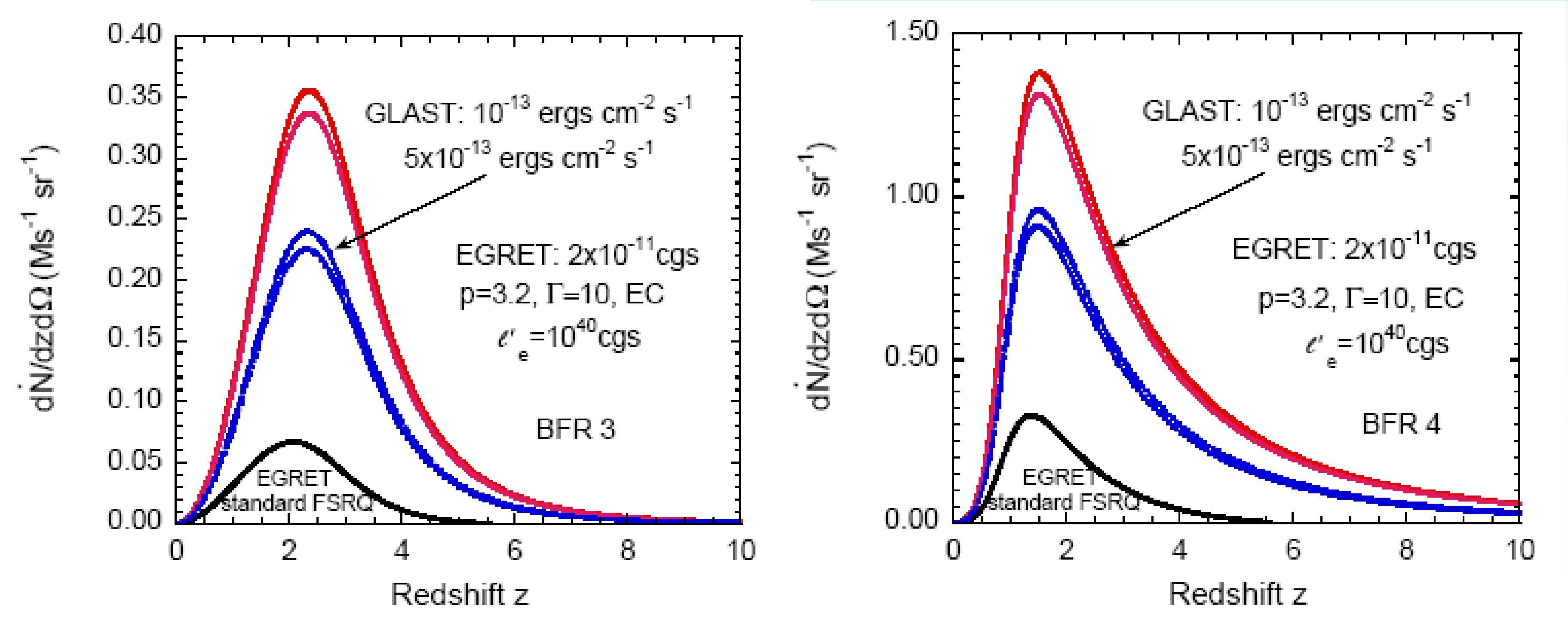

Fig. 8.— Model FSRQ redshift distribution for a standard model blazar with $\Gamma = 10$, EC statistics, and EGRET detection properties (upper blue dotted curve), for BFR 3 (left) and BFR 4 (right). GLAST predictions for $f_\epsilon^{thr} = 5 \times 10^{-13}$ ergs cm^{-2} s^{-1} and for $f_\epsilon^{thr} = 1 \times 10^{-13}$ ergs cm^{-2} s^{-1} are shown by the middle and upper pairs of curves, respectively. The observing frequency is $\epsilon = 200$ and $\epsilon = 2000$ for the higer and lower curve, respectively, in each pair of curves.

BLs not yet treated

GLAST Analysis of Blazars

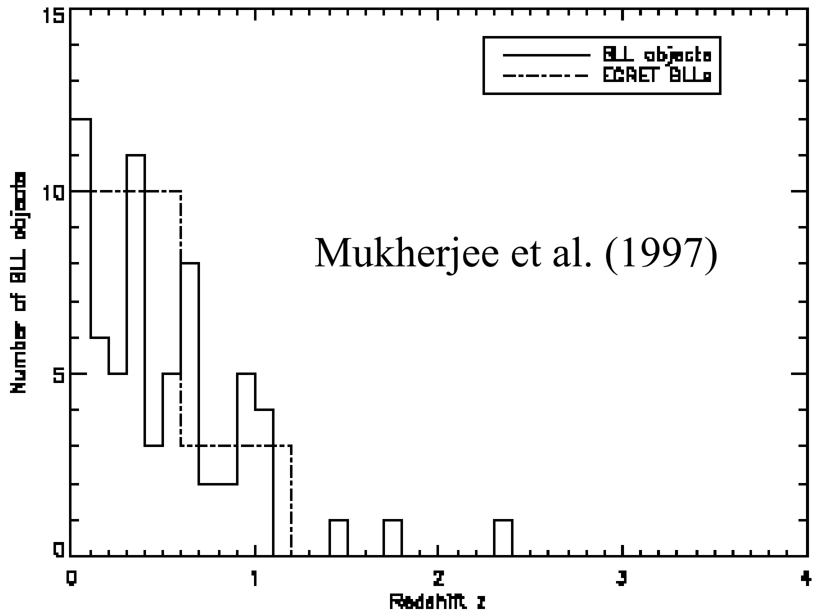

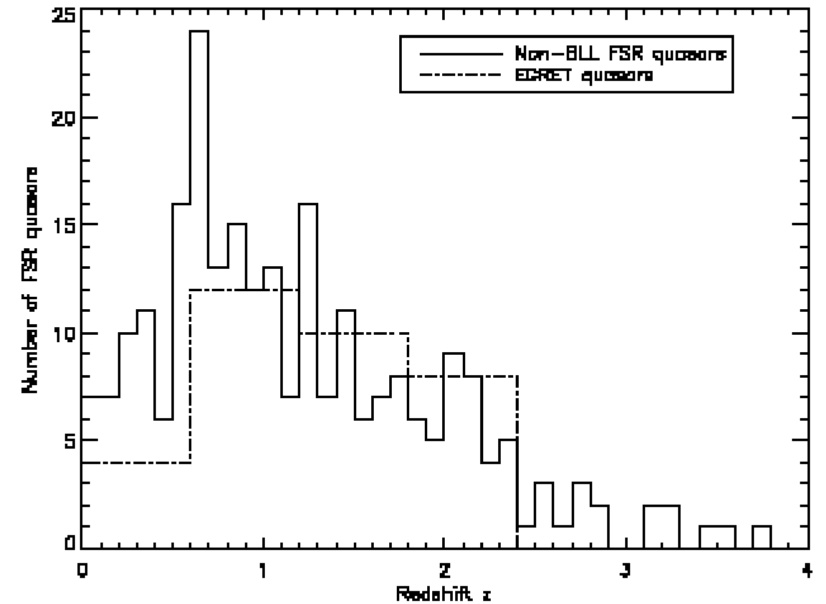

Measure three characteristic redshifts:

1. Average redshift <z> for entire sample
2. Average redshift <z_-> for z < <z>
3. Average redshift <z_+> for z > <z>

Determine characteristic redshifts for groupings by:

1. class type (most simply, FSRQ vs. BL)
2. Peak flux or average flux
3. Photon energy

Better analysis: Kolmogorov-Smirnov test

Compare with models:

1. Choose BFR, Statistics
2. Determine best values of Γ and ℓ'_e

   Degeneracy?

   Implications for parent pop?
3. Identify signatures of high-redshift blazars (e.g., $\gamma\gamma$ high-frequency dropouts)

Theoretical Basis for paper by Dermer and Davis (2000)

NB: Next 3 VGs are historical material, to be redone

Fit parameters for the FSRQs are Γ = 10 and comoving luminosity L= 3x10^{44} ergs s^{-1}; fit parameters for the BL Lacs are Γ = 5 and L = 5x10^{44} ergs s^{-1}.

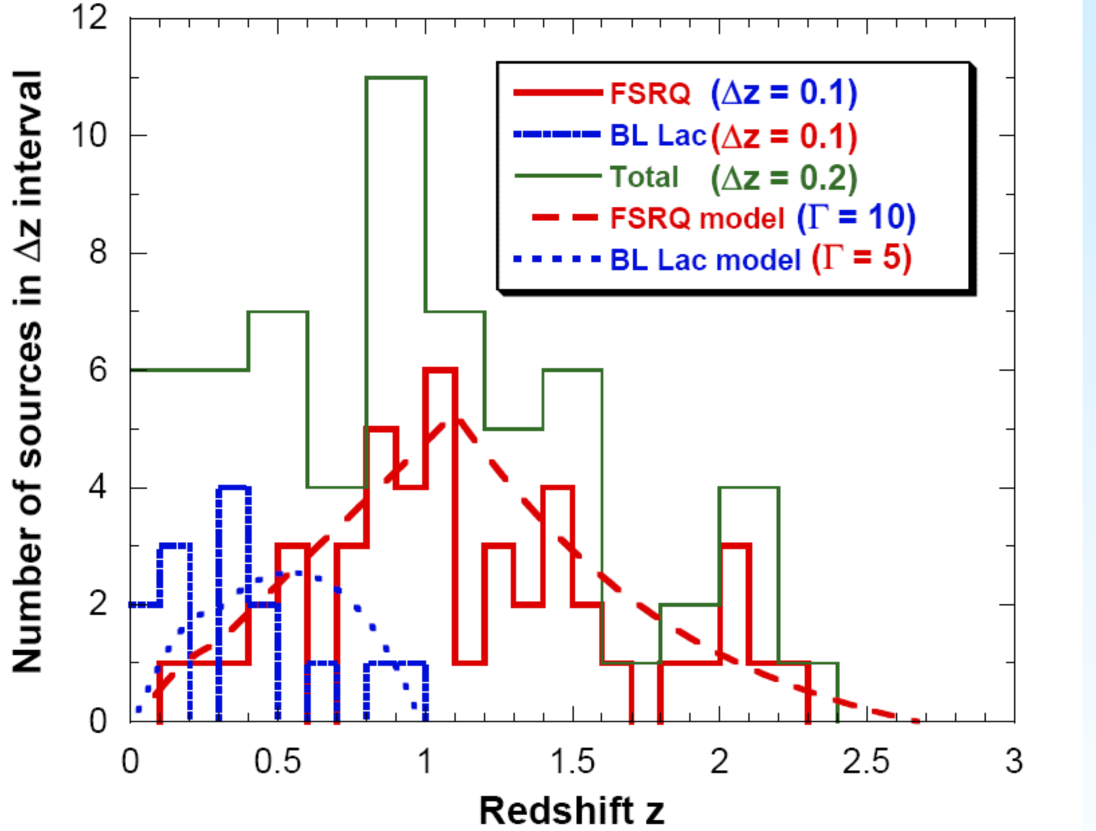

Fig. 1.— Redshift distribution of EGRET blazars (histograms) from the Third EGRET Catalog (3). Curves show model fits assuming comoving density proportional to the star formation rate (SFR; see Fig. 3b). Fit parameters for the FSRQs are $\Gamma = 10$ and comoving luminosity $L = 3 \times 10^{44}$ ergs s^{-1}; fit parameters for the BL Lacs are $\Gamma = 5$ and $L = 5 \times 10^{44}$ ergs s^{-1}.

(Peak) flux function of EGRET Blazars

Histogram showing the measured peak power flux size distribution of EGRET blazars, the fit to the size distribution with the model, and predictions for gamma-ray blazar detectibility with GLAST for a sensitivity threshold of $1.3\mathrm{x}10^{-12}$ ergs cm^{-2} s^{-1}

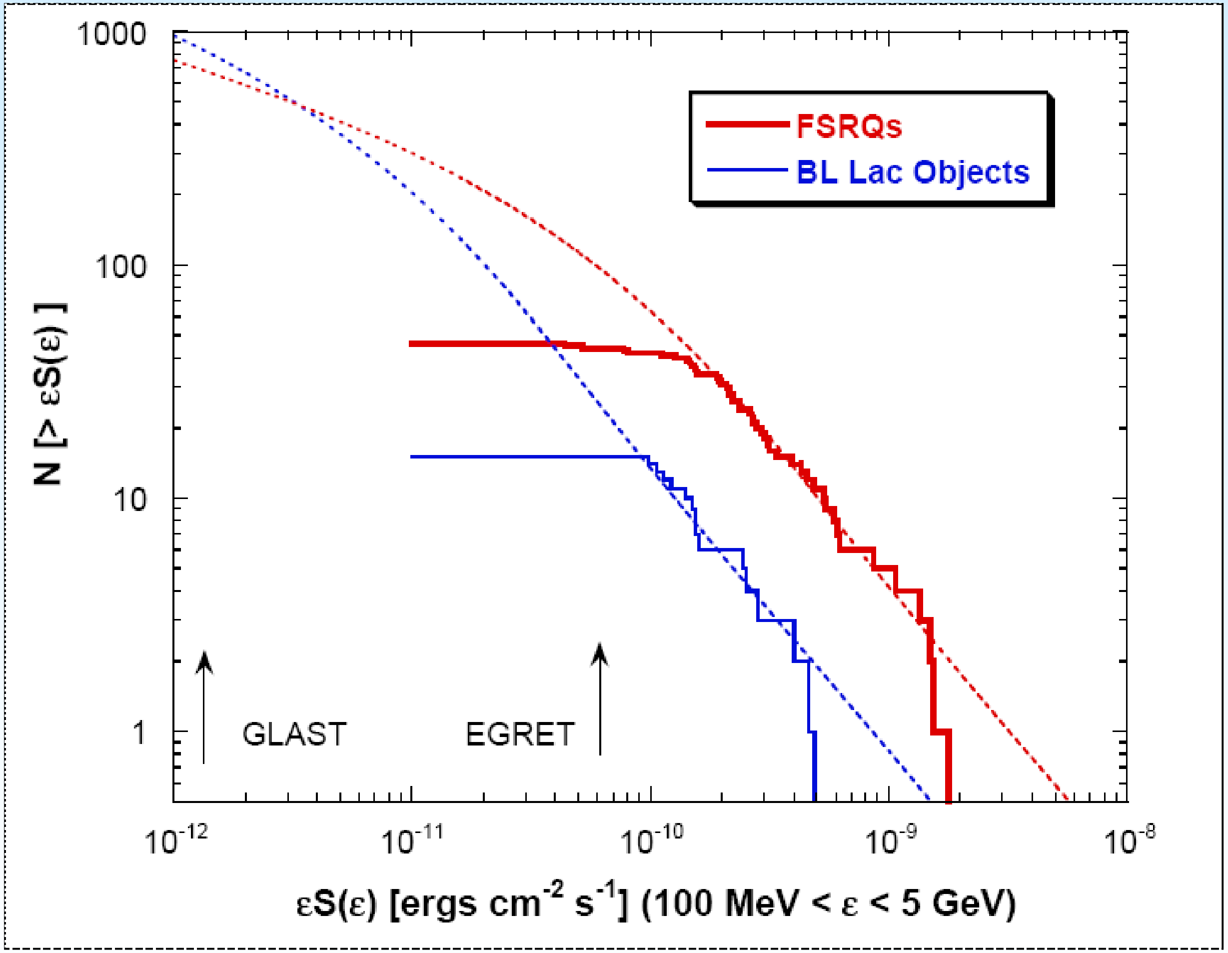

NB: GLAST is much more sensitive than this: but this preserves a ratio of 50:1 (GLAST vs. EGRET)

Predictions for GLAST

Predictions for the number of FSRQs and BLs to be detected with GLAST, assuming that the blazar rate follows the SFR history of the universe. Inset shows the range of high-redshift blazars implied by uncertainties in the SFR at large redshift

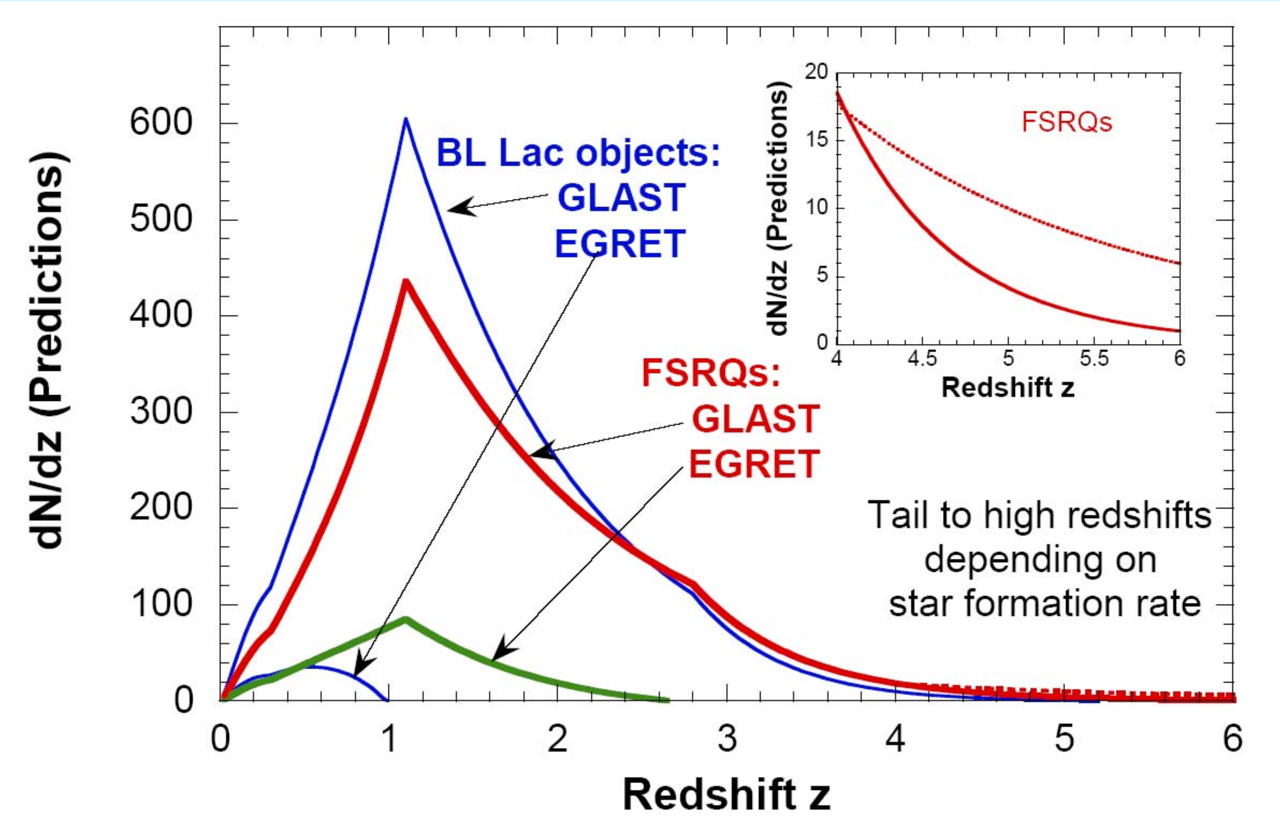

Diffuse γ-Ray Background

$$\epsilon I_\epsilon = \frac{c}{4\pi H_0} \int_0^\infty dz \oint d\Omega_* \frac{\epsilon_*^2\, q_{co}(\epsilon_*, \Omega_*; z)}{(1+z)^3 \sqrt{\Omega_m (1+z)^3 + \Omega_\Lambda}}$$

$$q_{co}(\epsilon_*, \Omega_*; z) = \frac{dN_\gamma}{d\epsilon_* dt_* dV_* d\Omega_*}$$

$$\epsilon_*^2 q_{co}(\epsilon_*, \Omega_*; z) = n_{co}(z) \epsilon_* J^s(\epsilon_*)$$

Subtract known point sources

Divide blazar class into persistent plus flaring component

Sreekumar et al. (1998)

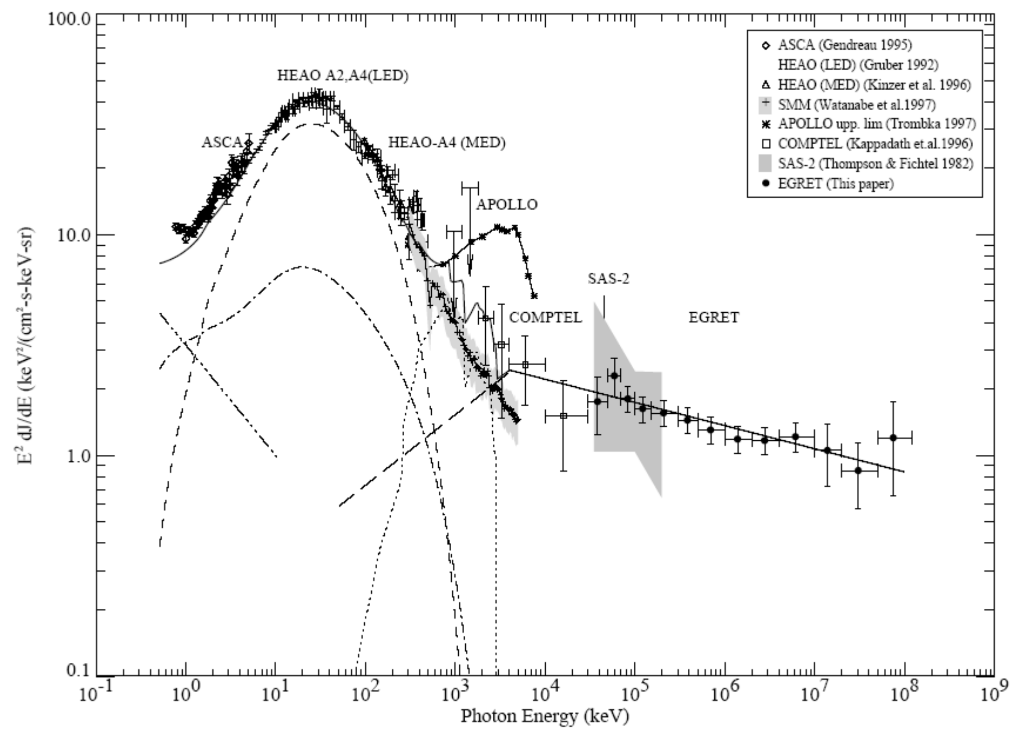

Redshift evolution of γ-ray blazars

Black Hole Activity through cosmic time

Relax assumption that

$$\Gamma(z) = \Gamma$$

$$\ell_e'(z) = \ell_e'$$

Feasible with GLAST observations

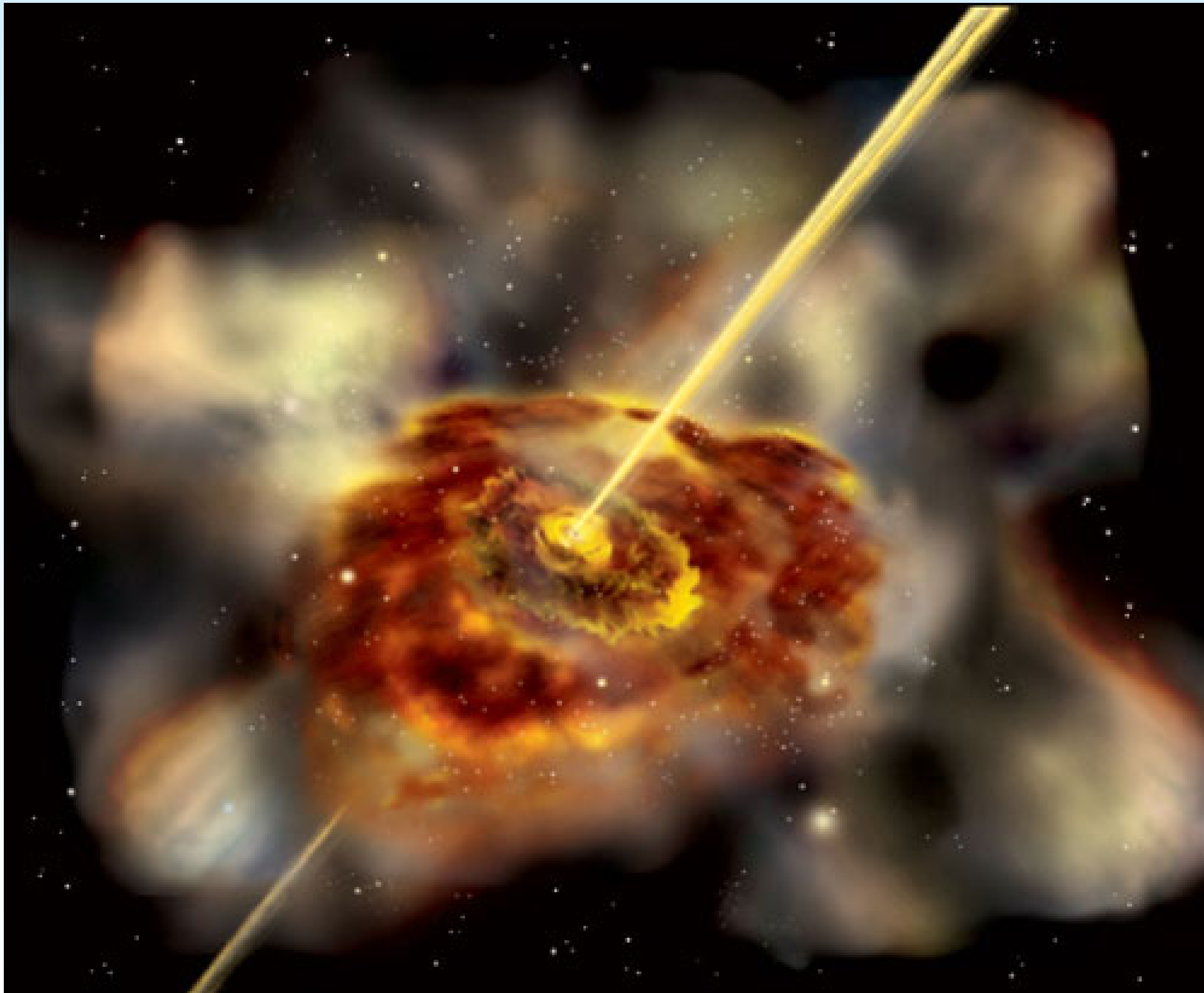

Summary: What we need from and for GLAST

- **Blazar catalogs and identification** (Romani et al.)

  a. Divide blazars into radio galaxies, BL Lac objects, LBL, and FSRQ (more or less BL Lac-like and FSRQ-like)

  b Divide blazar class into persistent plus flaring component

  c. Host galaxies of blazars: cosmic evolution

- **Redshift distribution for different source classes, different peak-flux ranges:**

  Minimal analysis: calculate 3 characteristic redshifts, compare with models

  Better analysis: KS comparison

- **Peak flux size distribution for different source classes, different redshift ranges**

- **Prediction: GLAST will see a larger ratio of BL Lacs/FSRQs than EGRET**

Cosmic evolution of supermassive black holes **(tracks IR rather than SFR?)**
Highly-evolved structure formation in early universe
Highest redshift persistent and persistently flaring sources
EBL

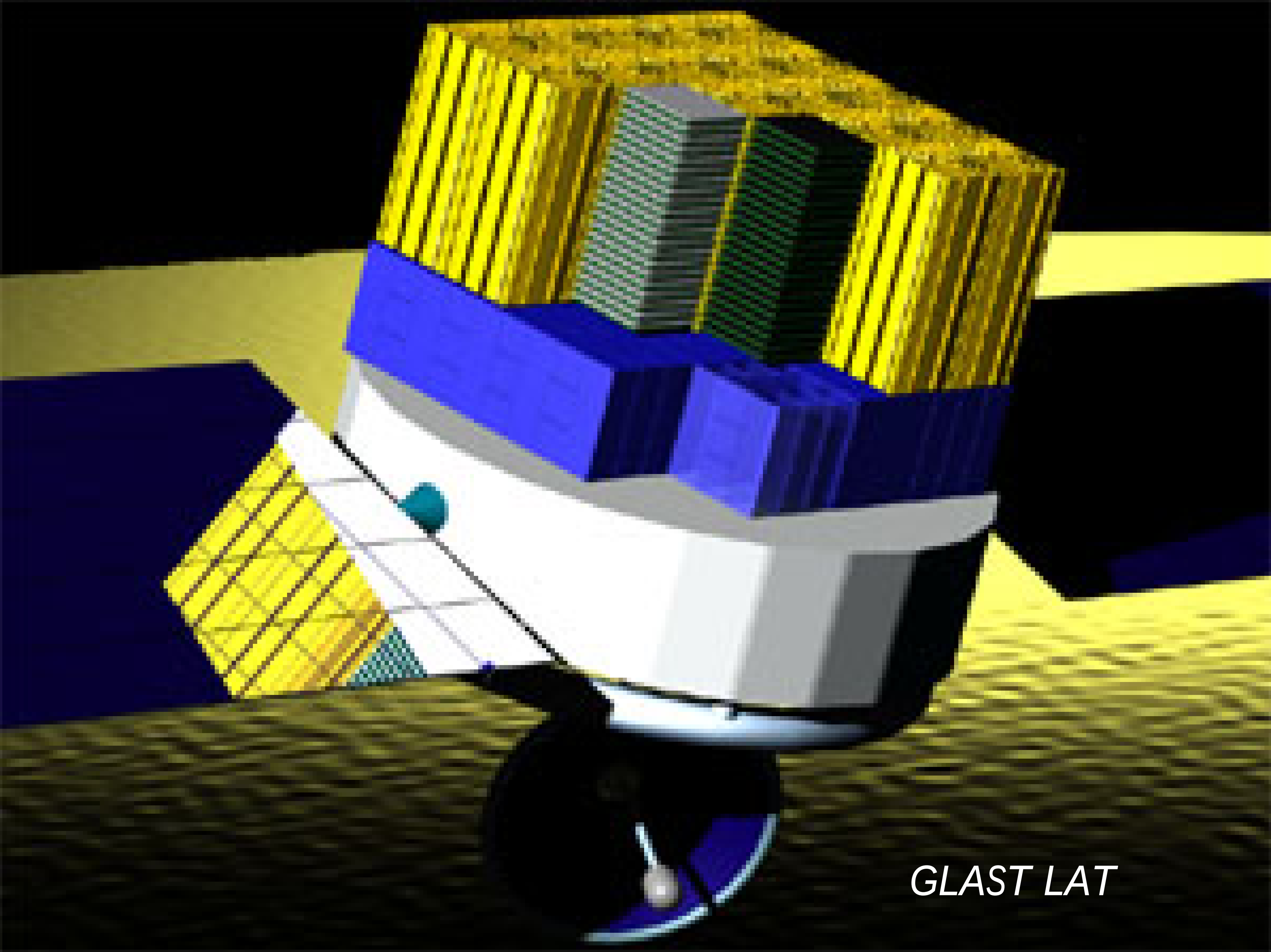
GLAST LAT